Binding Geometries of Benzo[*a*]pyrene Diol Epoxide Isomers Covalently Bound to DNA. Orientational Distribution†

Magdalena Eriksson,‡ Bengt Nordén,*,‡ Bengt Jernström,§ and Astrid Gräslund‖

Department of Physical Chemistry, Chalmers University of Technology, S-412 96 Göteborg, Sweden, Department of Toxicology, Karolinska Institutet, Box 60400, S-104 01 Stockholm, Sweden, and Department of Biophysics, Arrhenius Laboratory, University of Stockholm, S-106 91 Stockholm, Sweden

Received June 23, 1987; Revised Manuscript Received October 6, 1987

ABSTRACT: Flow linear dichroism (LD) of different benzo[*a*]pyrene diol epoxide (BPDE) isomers covalently bound to calf thymus DNA or poly(dG-dC) provides information about binding geometry and DNA perturbation. With *anti*-BPDE the apparent angle between the long axis (*z*) of the pyrene chromophore and the DNA helix axis is approximately 30° as evidenced from the LD of *z*-polarized absorption bands in the pyrenyl chromophore at 252 and 346 nm. The corresponding angle for the in-plane short axis (*y*) is determined to be approximately 70° from a *y*-polarized band at 275 nm. The binding of (+)-*anti*-BPDE to DNA is found to cause a considerable reduction of the DNA orientation. This is ascribed to a decreased persistence length of DNA, owing either to increased flexibility ("flexible joints") or to permanent kinks at the points of binding. The reduced linear dichroism (LD^r), i.e., the ratio between LD and isotropic absorbance, of the long-wavelength absorption band system of BPDE bound to DNA exhibits a wavelength dependence that indicates a relatively wide orientational distribution of the *z* axis of pyrene. Fluorescence data support the conclusion of a heterogeneous distribution, and a very low polarization anisotropy indicates a mobility between the different orientational states, which is rapid compared to the fluorescence lifetime (nanosecond time scale). Attempts are made to simulate the observed LD^r features of the (+)-*anti*-BPDE–poly(dG-dC) complex using different distribution models on the assumption that the angular dependence of the spectral perturbation is due to dispersive interactions with DNA bases. The simulations indicate the existence of two major orientation fractions of the pyrene *z* axis: one larger fraction around 20° to the helix axis and a smaller one around 70°. The result is discussed in terms of two interchangeable conformations of the covalent (+)-*anti*-BPDE–poly(dG-dC) complex.

Polyaromatic hydrocarbons like benzo[*a*]pyrene (BP) are common environmental contaminants and potential human carcinogens. The BP itself is not active as a carcinogen, but in biological systems it can be metabolically converted to highly reactive so-called bay-region diol epoxides that subsequently covalently attack specific targets on DNA (Gelboin, 1980; Conney, 1982; Cooper et al., 1982). The diastereomeric *trans*-7,8-dihydroxy-9,10-epoxy-7,8,9,10-tetrahydrobenzo[*a*]pyrene (BPDE) appears in four isomers: the (+)- and (−)-enantiomers of *syn*- and *anti*-BPDE. All of them have been shown to react covalently with DNA (Jeffrey, 1985). (+)-*anti*-BPDE is known to exhibit a high carcinogenic potency, while the other isomers are only moderate or weak tumorigens (Buening et al., 1978; Slaga et al., 1979). The (+)-enantiomer has a higher affinity for DNA than its (−)-analogue and the syn isomers (Meehan & Straub, 1979; Jeffrey, 1985) and exhibits a greater specificity for deoxyguanosine (Straub et al., 1977; Brookes & Osborne, 1982). The (+)-*anti*-BPDE addition occurs trans to the epoxide C-10 of BPDE to the exocyclic amino group of guanine (N-2) (Koreeda et al., 1978; Weinstein et al., 1978), which is localized in the minor groove of DNA. The occurrence of this adduct can be correlated to the tumour incidence in susceptible animals (Pelling & Slaga, 1982; Alexandrov et al., 1983; Nakayama et al., 1984; Pelling et al., 1984).

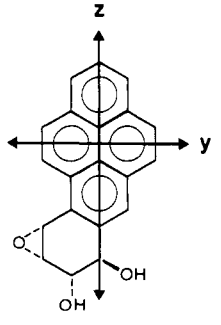

(+)-*anti*-BPDE

The BPDE isomers not only differ in biological activity, they also display stereochemical and spectroscopic differences in their DNA complexes. According to their spectroscopic properties the BPDE–DNA adducts have been divided into two types (Geacintov et al., 1982; Undeman et al., 1983; Jernström et al., 1984). The "type I adduct" is characterized by a negative linear dichroism (LD), a 10-nm shift toward longer wavelengths of the 300–350-nm absorption band system of the pyrenyl chromophore, and a strong fluorescence quenching [the fluorescence yield is approximately 0.03 of that of free benzo[*a*]pyrenetetraol in aqueous solution (Jernström et al., 1984)]. The spectroscopic properties of the type I adduct are similar to those of physical DNA complexes with common intercalators. The "type II adduct" exhibits a positive LD, and the absorbance red-shift is only 2–3 nm. Racemic *syn*-BPDE predominantly (~65%) forms type I adducts with DNA (Undeman et al., 1983), whereas (−)-*anti*-BPDE binds less specifically; about equal amounts of type I and type II

† This study was supported by grants from The Swedish Natural Science Research Council, Magn. Bergwalls Stiftelse, The Swedish Work Environmental Fund, and the Swedish Cancer Society.

* Author to whom correspondence should be addressed.
‡ Chalmers University of Technology.
§ Karolinska Institutet.
‖ University of Stockholm.

0006-2960/88/0427-1213$01.50/0

adducts are formed (Jernström et al., 1983; Geacintov et al., 1984). The (+)-*anti*-BPDE–DNA adducts can be characterized as being more than 90% type II.

The understanding of the two types of binding as to the structural details is still far from complete. The type I adduct is considered to have an essentially intercalative geometry, but steric constraints imposed by the covalent linkage and a measurable deviation from coplanarity with the DNA bases (~30°, Geacintov et al., 1982; Undeman et al., 1983) imply that there are considerable differences from a classical intercalation complex [the term "quasi-intercalation" is used by Geacintov et al. (1984)]. For the type II adduct an external binding mode, with the pyrenyl group residing in the minor groove, has been proposed by Geacintov et al. (1978). On the basis of an observed decrease in electric field induced DNA orientation after *anti*-BPDE binding, Hogan and co-workers have suggested a complex in which the BPDE acts like a wedge between two base pairs and thereby forces the DNA to bend some 30° (Hogan et al., 1981). In a previous paper (Eriksson et al., 1986) we presented LD results on the DNA interaction with (±)-*anti*-BPDE, for which it can be anticipated that the modification is mostly due to the (+)-enantiomer, representing the type II binding. An apparent binding angle of approximately 30° between the long axis of the pyrene chromophore and the DNA helix axis was obtained, in agreement with previous conclusions from electric and flow dichroism (Geacintov et al., 1978; Undeman et al., 1983). In addition, it was also possible to determine the angle of the pyrene short axis, ~70°, for this type II complex (Eriksson et al., 1986).

Apart from the effects of BPDE–DNA interaction locally at the binding site, an important question concerns the possible existence of long-range effects on the DNA conformation and stability. Observations of relevance for this question have been made in earlier studies on the B to Z conformational transition in poly(dG-dC). The results indicate that (+)-*anti*-BPDE adducts even at small binding ratios significantly influence the kinetics of the transition (Chen, 1985; Lycksell et al., 1985).

The strong carcinogenic potency of the (+)-*anti*-BPDE isomer, in combination with the observed unique structural properties of its covalent DNA adduct (the type II adduct), makes this isomer and its DNA interactions highly relevant to study, since DNA binding can be considered crucial for tumor initiation. The high binding preferentiality for guanine makes the pure polynucleotide poly(dG-dC) modified with (+)-*anti*-BPDE a particularly interesting system, thereby minimizing chemical heterogeneity. Previously reported variations of the reduced linear dichroism with wavelength, in the 300–350-nm wavelength band of BPDE–DNA complexes, which have been generally ascribed as an effect of heterogeneously oriented BPDE chromophores (Geacintov et al., 1978), are also observed in the (+)-*anti*-BPDE–poly(dG-dC) system. In the present study we will concentrate on interpreting these dichroism features in structural and dynamical terms.

It will be shown that the variations in LD^r of the absorption band of the long axis oriented pyrene transition can reveal detailed information about the geometrical heterogeneity of the (+)-*anti*-BPDE binding to poly(dG-dC). Hitherto, orientational conclusions based on dichroic measurements have been mainly restricted to apparent angles, assuming identical orientations for all chromophores [although the question of angular distribution has also been discussed previously (Geacintov et al., 1978)].

In addition we will address the question whether the concluded orientational distribution is of a static nature due to binding heterogeneity or of a dynamic nature, reflecting the mobility of the BPDE adduct. Conclusions regarding the mobility of the pyrene chromophore as well as the DNA flexibility are made from fluorescence measurements and the LD characteristics in the DNA absorption bands. The results on the (+)-*anti*-BPDE adduct in poly(dG-dC) consistently support the idea of an orientational distribution over two favored binding conformations, in equilibrium with one another, and with a rapid interchange between the two (on the nanosecond time scale of fluorescence lifetimes).

Materials and Methods

Chemicals. Racemic *syn*- and *anti*-BPDE and the separate enantiomers of the latter (>95% pure) were obtained through the Cancer Research Program of the National Cancer Institute, Division of Cancer Cause and Prevention, Bethesda, MD. The compounds were stored in dry tetrahydrofuran/triethylamine (19:1 v/v) at −20 °C. Immediately prior to use, the amount of BPDE solution required was freed of solvent by nitrogen purging and the residue dissolved in dry dimethyl sulfoxide. The concentration of the BPDE diastereomers was estimated from light absorbance at 343 nm by using a molar absorptivity of 49 700 M^{-1} cm^{-1} (the value was obtained from Chemical Repository, National Cancer Institute, Bethesda, MD). Calf thymus DNA and double-stranded alternating poly(dG-dC) were obtained from Pharmacia, Uppsala, Sweden. Prior to use, calf thymus DNA was further purified by treatment with proteinase K (Boehringer Mannheim Scandinavia, Bromma, Sweden), RNase (Sigma Chemical Co., St. Louis, MO), and phenol extraction as previously described (MacLeod & Zachary, 1985). The concentration of poly(dG-dC) and calf thymus DNA was estimated from light absorbance at 258 nm by using molar absorptivities of 8400 and 6600 M^{-1} cm^{-1}, respectively. All other chemicals used were of analytical grade.

Covalent Binding of BPDE to Calf Thymus DNA and Poly(dG-dC). BPDE was reacted with deproteinized calf thymus DNA or poly(dG-dC) for 60 min at 37 °C. One milliliter of the reaction mixture contained 10 OD_{258} of polynucleotides, 25–500 nmol of BPDE isomers dissolved in 25 μL of dimethyl sulfoxide, and 10 μmol of sodium cacodylate adjusted to pH 7.0 with HNO_3. Noncovalently bound BPDE or its hydrolysis products were removed by extensive extraction with buffer-saturated ethyl acetate as previously described (Undeman et al., 1983). The extent of covalent modification was quantified by light absorbance at 345 [(±)-*anti*-BPDE] or 353 nm [(±)-*syn*-BPDE] by using molar absorptivities of 29 000 M^{-1} cm^{-1} for both diastereomers (Pulkrabek et al., 1977).

Linear Dichroism. Linear dichroism (LD) is defined at any wavelength as the differential absorption between orthogonal forms of linearly polarized light

$$LD(\lambda) = A_{\parallel}(\lambda) - A_{\perp}(\lambda) \quad (1)$$

where ∥ and ⊥ denote polarization of the electric field of light parallel and perpendicular to the orientation direction (flow direction). Light is propagated radially through the concentric silica cylinders of a Couette cell of Wada type (Wada & Kozawa, 1964), and the LD is measured differentially by using polarization modulation in a modified commercial circular dichrometer (Jasco J-500) as described before (Davidsson & Nordén, 1976) [for calibration, see Nordén and Seth (1985)]. The LD is normalized to be independent of concentration and path length through division by the isotropic absorbance, A_{iso} (measured on a wavelength-matched Cary 219 spectrophotometer), to form the reduced linear dichroism, LD^r:

$$LD^r(\lambda) = LD(\lambda)/A_{iso}(\lambda) \quad (2)$$

LD^r can be related to the orientation of the absorbing transition moments according to (Nordén, 1978)

$$LD^r(\lambda) = \frac{\sum_i Q_i \epsilon_i(\lambda)(LD^r)_i}{\sum_i Q_i \epsilon_i(\lambda)} \quad (3a)$$

$$(LD^r)_i = {}^3/_2 S(3\langle\cos^2 \alpha_i\rangle - 1) \quad (3b)$$

where $\epsilon_i(\lambda)$ is the decadic extinction coefficient of component i at wavelength λ, Q_i is its fractional concentration, and S is an orientation factor for a local helix axis of DNA. $S = 1$ denotes perfect orientation parallel to the flow direction and $S = 0$ random orientation. α_i is the angle between the transition moment i and the helix axis. Note the distinction between the true α values (which may be heterogeneously distributed) and the "apparent" angles calculated in LD experiments from the measured second moments $\langle\cos^2 \alpha\rangle$ (see definition in Table I). An effective $\alpha_{DNA} = 86°$ for 260 nm (several contributing transitions) has been determined for the B-form fiber DNA (Matsuoka & Nordén, 1982a). For a given steady-state orientation S can be determined, according to eq 3b, from the LD^r measured at 260 nm after a (generally small) correction for the BPDE absorption.

Assuming that S represents the average orientation of the DNA helix, also for the part where BPDE is bound, a value of $\langle\cos^2 \alpha\rangle$ and a corresponding apparent angle α can be determined from the measured LD^r of an absorption band of BPDE of known polarization through reuse of eq 3b (see also Table I). In BPDE, and in its complex with DNA, the active chromophore is pyrene, owing to the saturated character of the epoxycyclohexanediol ring.

If perturbation of the polarization directions of the pyrene chromophore due to substituents may be neglected [as seems justifiable from spectroscopic evidence (Langkilde et al., 1977)] any $\pi\pi^*$ transition must be polarized along either of the two symmetry axes, denoted y and z. The resolved, pure y- and z-polarized spectra of pyrene are shown at the top of Figure 1 (Thulstrup et al., 1977). The orientation of the z axis of BPDE (α_z) can be readily determined from measurement of LD^r (346 nm) of the flow-oriented BPDE–DNA complex [and simultaneous measurement of LD^r (260 nm)], whereas the determination of the orientation of the y axis (α_y) requires subtraction of the overlapping DNA absorption for obtaining the contribution to LD^r (275 nm) from BPDE. A resulting relatively well-reproduced pyrene spectrum, in both LD and A_{iso}, justifies the assumption that the polarizations and absorption intensities of BPDE, also in its complex with DNA, are roughly the same as in the unsubstituted pyrene chromophore.

Fluorescence. Fluorescence was measured on an Aminco SPF-500 spectrofluorometer ("corrected spectra"). Fluorescence polarization anisotropy (FPA) was determined by inserting polaroids in the excitation and emission paths. FPA is defined as $FPA = (I_\parallel - I_\perp)/(I_\parallel + 2I_\perp)$, where $I_\parallel$ and $I_\perp$ denote the intensities of the steady-state fluorescence polarized parallel and perpendicular to the vertically polarized exciting light. For a totally rigid system of immobile chromophores, the anisotropy exhibits a maximum value of +0.4, provided the absoring and emitting transition moments are parallel. In the case in which these transitions are orthogonal to one another, a minimum FPA value of –0.2 is expected for immobile chromophores (Cantor & Schimmel, 1980).

Simulation of Spectra. The LD^r spectra are simulated under the assumption that the variation of $LD^r(\lambda)$ with wavelength of the 300–350-nm vibrational progression is due to inhomogeneous broadening [this is the mechanism denoted "Case III:b" by Geacintov et al. (1978)]. It is further assumed that the spectral shift of the BPDE absorption is caused by a nondegenerate coupled-oscillator interaction with the transitions of the DNA bases. The strongest interaction (largest red-shift) is expected when the pyrene chromophore is parallel to the planes of the DNA bases. The effect of a heterogeneous distribution can be visualized as follows. Imagine two fractions of BPDE molecules, one oriented parallel to the helix axis (absorbing at short wavelengths) and one parallel to the DNA bases (absorbing at longer wavelengths). The resulting absorption spectrum will now show a broadening compared to the chromophore in a homogeneous environment, and the linear dichroism, in this extreme example, will display a positive feature at the short-wavelength side of the absorption band and a negative one at the long-wavelength side, corresponding to the two fractions of differently oriented chromophores. Owing to its differential nature, LD^r will thus more sensitively than absorption broadening reflect an inhomogeneous orientation of BPDE chromophores.

In the simulations of LD^r we have applied an approximate relation for the angular dependence of the wavelength shift $\Delta\lambda$ (see Appendix)

$$\Delta\lambda = \Delta\lambda^{solv} + \Delta\lambda^\circ \sin \alpha \quad (4)$$

where $\Delta\lambda^{solv}$ and $\Delta\lambda^\circ$, defined in the Appendix, are gauged experimentally. α is the angle between the transition moment of the pyrene chromophore and the DNA helix axis. In our calculations we have used $\Delta\lambda^{solv} = 3$ nm and $\Delta\lambda^\circ = 12.5$ nm by inference from the shifts observed for the type I and type II BPDE–DNA complexes and comparison with free BPDE in ethanol.

The orientational distribution of the pyrene z axis relative to that of the DNA helix axis (angle α) will be described by a normalized frequency function, $F(\alpha)$, for a couple of simple model distributions. A general integrable distribution $F(\alpha)$ is first truncated by defining upper and lower limiting angles α^+ and α^-, respectively. The angular range $\alpha^+ - \alpha^-$, outside which F is neglected, is then divided into n equal intervals of an angular width $\Delta\alpha = (\alpha^+ - \alpha^-)/n$. The center of the angular range is denoted $\alpha_0 = (\alpha^+ + \alpha^-)/2$. For each interval a characteristic angle (α_i) will be used, defined as $\alpha_i = \alpha^- + (i - {}^1/_2)\Delta\alpha$, as well as its fractional contribution (Q_i) to the distribution:

$$Q_i = \int_{\alpha_i - 0.5\Delta\alpha}^{\alpha_i + 0.5\Delta\alpha} F(\alpha)\, d\alpha \quad (5)$$

For a Gaussian distribution

$$F(\alpha) = (2\pi)^{-1/2} \exp\{-0.5[(\alpha - \alpha_0)/\sigma]^2\} \quad (6)$$

with σ the standard deviation, the reduced linear dichroism spectrum can be calculated as

$$LD^r(\lambda) = \frac{\sum_{i=1}^{n} Q_i \epsilon(\lambda + \Delta\lambda_i)(LD^r)_i}{\sum_{i=1}^{n} Q_i \epsilon(\lambda + \Delta\lambda_i)} \quad (7a)$$

with

$$(LD^r)_i = {}^3/_2 S(3\cos^2 \alpha_i - 1) \quad (7b)$$

with S, the orientation factor, determined by the use of eq 3b on the DNA absorption band as described earlier. Note the different definitions of $(LD^r)_i$ in eq 3 and 7 (in eq 3 it is the LD^r contribution from one transition, averaged over the whole

Table I: Apparent Binding Angles

determined for	polarization	α_i[a] (deg)
anti-BPDE–DNA		
346 nm	z	34
275 nm	y	75
252 nm	z	33
(+)-*anti*-BPDE–poly(dG-dC)		
346 nm	z	26

[a] Apparent angle defined as arc cos $[\langle\cos^2 \alpha_i\rangle]^{1/2}$ (Nordén & Seth, 1979), with $\langle\cos^2 \alpha_i\rangle$ obtained according to eq 3.

orientational distribution, while in eq 7 it refers to a single angular element of the distribution).

Results

Linear Dichroism. In Figure 1 representative LD and A_{iso} spectra, as well as LD^r spectra, are shown for *anti*-BPDE–DNA (contributions from DNA depicted by broken curves in Figure 1b,c). LD^r spectra of pure DNA and of the complexes with (±)-*syn*-, (+)-*anti*-, and (−)-*anti*-BPDE are also shown in Figure 1d. Important observations are the positive, similar LD^r amplitudes of *anti*-BPDE at 310–350 nm and at 235–255 nm, corresponding to pure z-polarized pyrene transitions, and the negative LD^r of the y-polarized 275-nm pyrene absorption band. Compare Figure 1a that shows the pure resolved polarized spectra of pyrene as determined from stretched-film measurements. The corresponding apparent angles α_z (long axis) and α_y (short axis), obtained according to eq 3 from the respective LD^r values [including the use of LD^r (260 nm) of DNA for determining S] are summarized in Table I. The long axis of the DNA-bound pyrene chromophore is, according to this interpretation, oriented nearly parallel to the helix axis ($\alpha_z \sim 30°$), whereas the in-plane short axis tends to be more perpendicularly oriented ($\alpha_y \sim 70°$).

The pure polarization (parallel to z) of the 300–350-nm absorption region of the pyrene chromophore would result in a constant LD^r if all molecules were identically oriented. Therefore, the pronounced variation in LD^r between 300 and 350 nm implies an orientational distribution of the bound BPDE chromophores at different angles. This feature is observed for all of the BPDE isomers when bound to DNA (Figure 1e) and also for the (+)-*anti*-BPDE–poly(dG-dC) adduct, as will be discussed below (Figure 4).

When the binding ratio, r (=BPDE–adduct/DNA nucleotide), is increased, the shape of the LD^r spectrum is essentially unchanged but its amplitude is considerably decreased [shown for $r = 0.025$ and $r = 0.0096$, parts d and e of Figure 1, respectively, for (±)-*anti*-BPDE]. In Figure 2 it is seen that the LD^r values at 260 and 346 nm exhibit similar dependences on the binding ratio; i.e., the ratio $LD^r(346)/LD^r(260)$ is approximately constant (Figure 2b). As will be inferred, this indicates a lower degree of orientation of DNA (a lower S) after the (+)-*anti*-BPDE is bound. The reduction in DNA orientation appears to be less pronounced for the (−)-*anti*- and (±)-*syn*-BPDE–DNA complexes both at 260 and 350 nm (Figure 2a). These isomers form predominantly type I adducts with intercalative properties and may therefore rather be expected to enhance the orientability of DNA.

Simulations. Attempts to simulate the LD^r spectra were made as described under Materials and Methods. Figure 3a defines three parameters used for characterizing the spectral features of LD^r in the 310–350-nm absorption region of BPDE: the average amplitude, $\langle LD^r\rangle$, the peak-to-trough amplitude, $LD^r_{p/t}$, and the bandwidth, $\Delta\lambda_{1/2}$. Four model distributions were applied: (I) "single Gaussian"; (II) "two-state"; (III) "double Gaussian"; and (IV) "limited isotropic domain" model

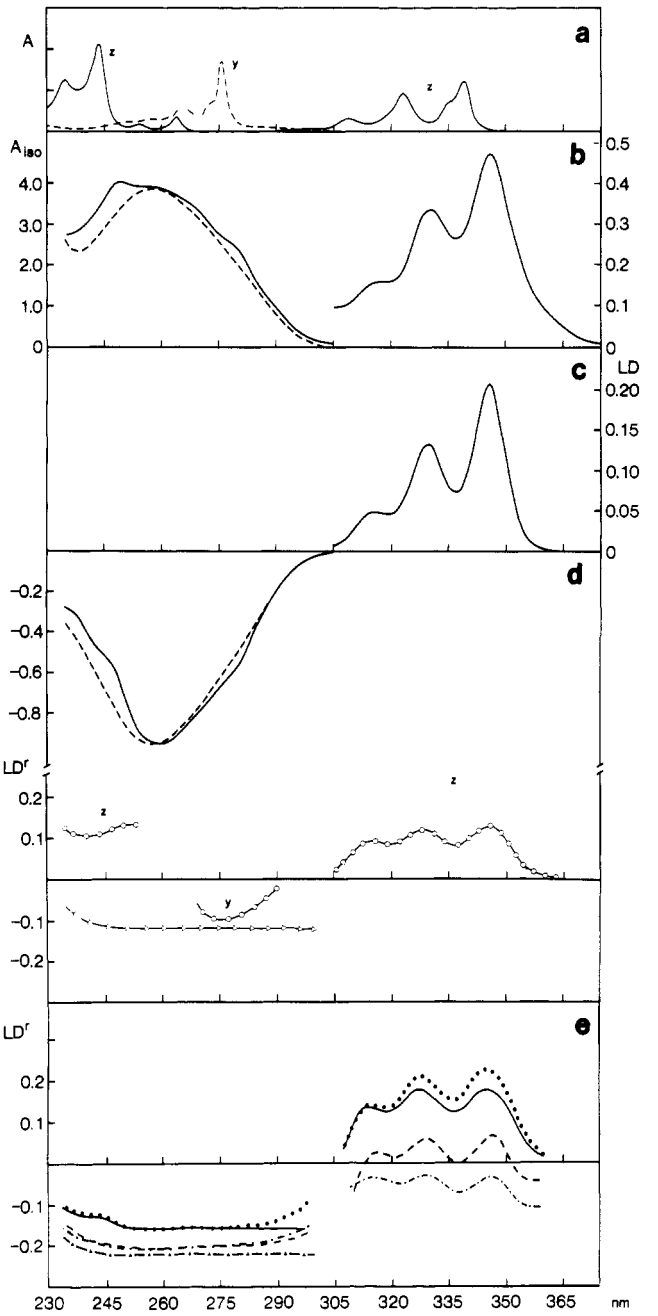

FIGURE 1: (a) Polarized component spectra of the pyrenyl chromophore: solid and broken curves refer to z- and y-polarized absorption components, respectively, as obtained for pyrene in polyethylene matrix (Thulstrup et al., 1977). (b,c) Isotropic absorbance and linear dichroism spectra of *anti*-BPDE–DNA (0.59 mM phosphate, $r = 0.025$) (solid curve) and of pure DNA (broken curve). (d) Resolved LD^r components: pyrenyl chromophore (○); DNA chromophore (△). (e) LD^r spectra of (+)-*anti*-BPDE–DNA (···) ($r = 0.0067$), (±)-*anti*-BPDE–DNA (—) ($r = 0.0096$), (−)-*anti*-BPDE–DNA (- - -) ($r = 0.0037$), and (±)-*syn*-BPDE–DNA (-·-) ($r = 0.0060$). LD^r spectrum of unmodified DNA (▲).

distribution. The distributions, $F(\alpha)$, and the parameters applied are presented in Table II. The two-state distribution consists of two Δ functions at $\alpha = \alpha_1$ and α_2 with fractional contributions Q_1 and Q_2, respectively. The double-Gaussian means two Gaussian distribution functions, according to eq 6, centered at two different angles α_0. For the limited isotropic domain distribution, $F(\alpha)$ is constant in a given angular range. A few examples of the distributions are shown in Figure 3b. Representative results of the simulations are in Figure 4 (and Table II) compared to the experimental LD^r spectra of (+)-*anti*-BPDE bound to poly(dG-dC).

Table II: Orientational Distribution Models. Characteristic Data

distribution model	$LD^r_{p/t} \times 10^3$	$\langle LD^r \rangle$	$\Delta\lambda_{1/2}$
(I) single Gaussian[a]			
(1) $\alpha_0 = 20°$, $\sigma = 10°$	1.24	18.6	8.5
(2) $\alpha_0 = 30°$, $\sigma = 10°$	1.53	14.1	10.2
(3) $\alpha_0 = 25°$, σ 20°	4.24	14.7	10.2
(4) $\alpha_0 = 30°$, $\sigma = 20°$	4.87	12.7	10.8
(II) two state[b]			
(1) $\alpha_1 = 20°$, $Q_1 = 0.95$, $\alpha_2 = 70°$, $Q_2 = 0.05$	1.73	17.7	
(2) $\alpha_1 = 30°$, $Q_1 = 0.95$, $\alpha_2 = 70°$, $Q_2 = 0.05$	1.28	13.4	12.0
(3) $\alpha_1 = 20°$, $Q_1 = 0.70$, $\alpha_2 = 70°$, $Q_2 = 0.30$	7.01	10.6	11.0
(4) $\alpha_1 = 30°$, $Q_1 = 0.70$, $\alpha_2 = 70°$, $Q_2 = 0.30$	5.23	7.5	11.2
(III) double Gaussian[c]			
(1) $\alpha_0 = 20°$, $\sigma = 5°$, $\sum Q_i = 0.80$	5.74	13.5	10.5
$\alpha_0 = 70°$, $\sigma = 5°$, $\sum Q_i = 0.20$			
(2) $\alpha_0 = 20°$, $\sigma = 10°$, $\sum Q_i = 0.80$	5.85	13.1	10.8
$\alpha_0 = 70°$, $\sigma = 10°$, $\sum Q_i = 0.20$			
(3) $\alpha_0 = 20°$, $\sigma = 10°$, $\sum Q_i = 0.90$	3.82	15.8	11.2
$\alpha_0 = 70°$, $\sigma = 10°$, $\sum Q_i = 0.10$			
(4) $\alpha_0 = 15°$, $\sigma = 10°$, $\sum Q_i = 0.80$	5.95	14.8	11.0
$\alpha_0 = 65°$, $\sigma = 10°$, $\sum Q_i = 0.20$			
(IV) limited isotropic domain[d]			
(1) $\alpha^- = 0°$, $\alpha^+ = 90°$	7.41	6.0	10.2
(2) $\alpha^- = 20°$, $\alpha^+ = 70°$	3.39	5.7	10.2
(3) $\alpha^- = 10°$, $\alpha^+ = 50°$	2.28	13.9	10.5
(V) experimental[e]			
(+)-*anti*-BPDE–poly(dG-dC)	5.59	13.9	9.0

[a] Distribution $F(\alpha)$ according to eq 6; see also Figure 3b:I. [b] Two fractions Q_1 and Q_2 corresponding to α_1 and α_2 (see Figure 3b:II). [c] See Figure 3b:III. [d] See Figure 3b:IV. [e] See solid curve in Figure 4.

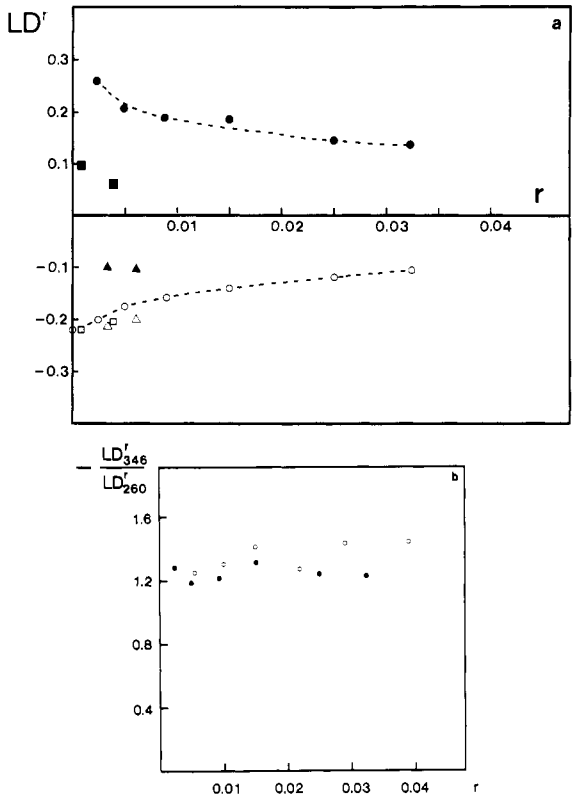

FIGURE 2: (a) Reduced linear dichroism of DNA and BPDE chromophores versus binding ratio for (±)-*anti*-BPDE–DNA at 260 (○) and 346 nm (●), for (−)-*anti*-BPDE–DNA at 260 (□) and 346 nm (■), and for (±)-*syn*-BPDE–DNA at 260 (△) and 355 nm (▲). (b) Ratio LD^r_{346}/LD^r_{260} for (±)-*anti*-BPDE–DNA versus r (filled and empty circles represent different sample series).

Fluorescence. Figure 5 presents fluorescence results on (+)-*anti*-BPDE bound to DNA. Excitation at two different wavelengths gives clearly different emission profiles (Figure 5a), indicating the presence of BPDE chromophores in different environments. Above 440 nm a broad shoulder can be assigned to fluorescence from excimers [compare the pyrene spectrum in Birks (1980)]. This indicates flexible attachment and closeness of the BPDE molecules. For the pyrene excimer the equilibrium distance between the chromophores is 3.4 Å (Birks, 1980). In Figure 5b measurements of fluorescence polarization anisotropy (FPA) are presented for excitation in both the z- and y-polarized absorption bands at 350 and 275 nm, respectively, at some different degrees of BPDE modification. Only very low (positive) FPA values were observed, indicating practically complete depolarization within the lifetime of the excited BPDE adduct.

Discussion

The present study provides information on the binding geometry of the BPDE–DNA complex on two levels. First, the short-axis polarized transition of the pyrene chromophore, resolved around 275 nm from the DNA absorption, adds a new dimension to the geometric information obtained from the long-axis transition around 350 nm. With the corresponding two apparent angles relative to the DNA helix axis, a three-dimensional, average geometry for the BPDE–DNA complex may be deduced. Second, and more interesting, the wavelength dependence of LD^r, supported by fluorescence results, can be consistently interpreted in terms of a dynamic orientational distribution of BPDE covalently linked to DNA.

Average Binding Geometry. Whereas the nearly parallel orientation of the long axis of (+)-*anti*-BPDE relative to the orientation of the helix axis has been established through both flow and electric LD measurements (Geacintov et al., 1978, 1984; Hogan et al., 1981; Undeman et al., 1983; Jernström et al., 1984), the short-axis orientation has until recently remained undetermined (Eriksson et al., 1986). The orientations of the long- and short-axes polarized transitions of *anti*-BPDE, bound to calf thymus DNA, as evidenced from the flow LD spectra, are shown in Table I. Calf thymus DNA was used because of its better flow orientation, compared to poly(dG-dC), which was required to obtain a detailed resolution of the LD spectrum. The similar orientations of the chromophore long axis in the adducts of DNA and poly(dG-dC) suggest that the orientation about 75° for the short axis applies also to (+)-*anti*-BPDE when bound to poly(dG-dC). It may be noted that a tilt of 30° of the long axis relative to the helix axis

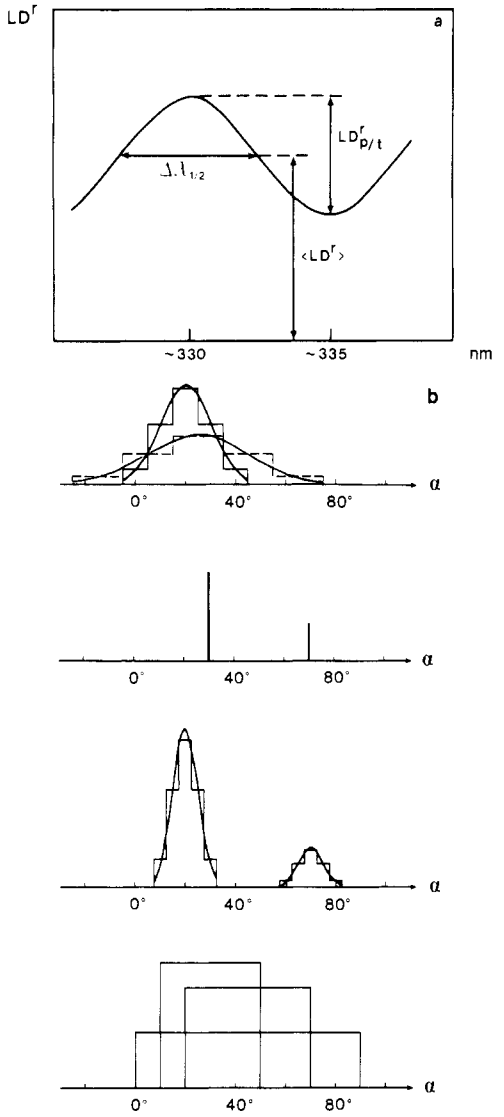

FIGURE 3: (a) Definitions of parameters characterizing the spectral features of LD^r in the 310–350-nm absorption region. (b) Examples of tested distributions (from top to bottom): single Gaussian (1 and 3 of Table II); two states (4 in Table II); double Gaussian (2 in Table II); limited isotropic domain (1, 2, and 3 in Table II).

restricts the short-axis orientation to 60°–90°. The presence of a fraction of intercalated BPDE adducts would make the short-axis angle virtually closer to 90°; the obtained value of 75° therefore excludes any larger fraction of intercalated BPDE.

Dependence of Orientation on Binding Ratio. Figure 2 contains information about the orientation of DNA as well as that of the BPDE adducts at different degrees of covalent modification. The decrease in LD^r_{260}, by approximately 30% at 1% modification with *anti*-BPDE, can be explained only by a considerably reduced persistence length owing to the introduction of kinks or "flexible joints" at the binding positions. The great change in LD^r observed at low binding ratios and the nonlinear variation with binding ratio exclude inclination of the DNA bases as an explanation for the behavior of LD^r_{260} in Figure 2.

Although (−)-*anti*-BPDE and (±)-*syn*-BPDE have lower affinities for DNA, and hence cannot be studied at the same high binding ratios as the (+)-*anti* isomer, the LD^r results indicate that they do not affect the DNA flexibility to the same extent. The difference may be ascribed to the different modes of binding of the isomers to DNA, a point we shall return to.

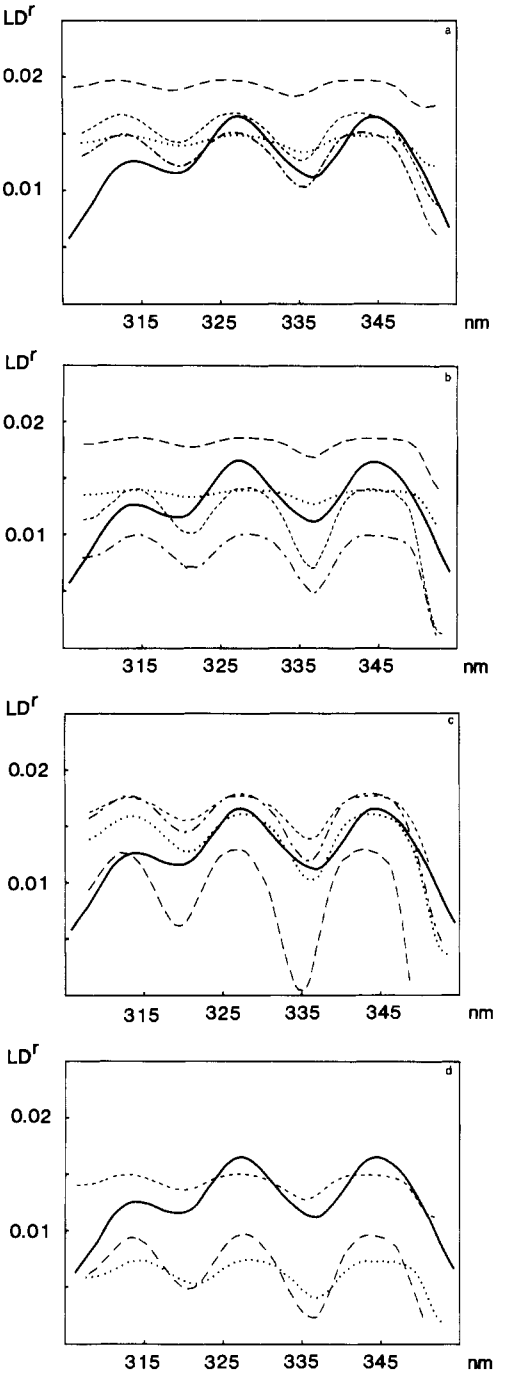

FIGURE 4: Simulated LD^r spectra of (+)-*anti*-BPDE bound to DNA, shown together with the experimental LD^r spectrum of (+)-*anti*-BPDE–poly(dG-dC) (—). The orientation distributions are defined in Figure 3b and Table II. (a) Single-Gaussian distribution I:1 (– – –), I:2 (···), I:3 (– · –), and I:4 (– · –). (b) Two-state distribution II:1 (– – –), II:2 (···), II:3 (– · –), and II:4 (– · –). (c) Double-Gaussian distribution III:1 (– – –), III:2 (···), III:3 (– · –), and III:4 (– · –). (d) Limited isotropic domain IV:1 (– – –), IV:2 (···), and IV:3 (– · –).

An important question is whether the orientation of the BPDE adduct varies with the degree of modification. This would be the case, for example, if there were two BPDE binding sites differing in affinity and orientation. A variation of the BPDE orientation with binding ratio would also be expected if the binding were cooperative, so that adjacent, interacting BPDE molecules get an orientation different from the BPDEs bound as isolated adducts. However, the practically constant ratio, LD^r_{346}/LD^r_{260}, over the range r = 0.002–0.032 indicates that there is no variation of the BPDE orientation relative to DNA in this binding range. The in-

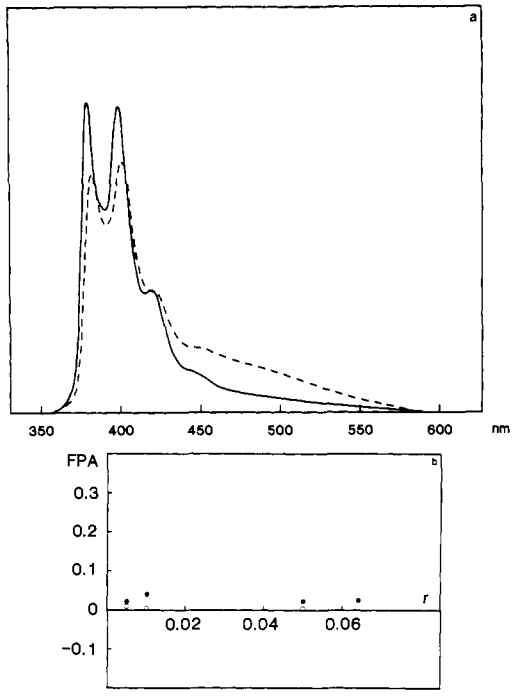

FIGURE 5: (a) Fluorescence emission spectra of (+)-*anti*-BPDE–DNA (0.33 mM phosphate). Excitation wavelengths: 340 (—) and 355 nm (---). Arbitrary fluorescence intensity units (vertical axis). (b) Fluorescence polarization anisotropy of (+)-*anti*-BPDE–poly(dG-dC). Emission wavelength 400 nm, excitation wavelengths 275 (○) and 350 nm (●).

variant spectral shape of LD^r (300–360 nm) of the *anti*-BPDE–DNA complex for $r = 0.0096$ and 0.025 also supports the conclusion that the average BPDE binding geometry does not measurable depend on the degree of modification. Hogan et al. (1981), from electric dichroism measurements, report that the limiting dichroism at 346 nm decreases more rapidly, with increasing degrees of modification, than does the limiting DNA dichroism. This is in conflict with our observation that the LD^r amplitudes of BPDE and DNA follow the same pattern (Figure 2b). We have no explanation for the difference but note that flow dichroism, since it can be measured with high accuracy at different wavelengths on the same sample, should be a more reliable method for determining relative orientations.

Origin of Wavelength Dependence in LD^r. LD^r, the ratio between the LD and the isotropic absorption spectrum, is constant in an absorption region if the absorbing transition moments are equally oriented or absorb at the same wavelengths. Thus, for a single transition, like in pyrene at 300–350 nm (Thulstrup et al., 1977), LD^r would be constant if the chromophore were oriented in a homogeneous environment [for example, in a stretched polymer film (Matsuoka & Nordén, 1982b)]. In a heterogeneous environment, a varying LD^r is expected if the chromophore is distributed over orientations that perturb the transition energy to different extents.

In DNA the interaction of planar molecules with the base-pairs is known to produce a shift toward longer wavelengths in the light absorption spectra of bound chromophores, as is clearly pronounced with intercalators (Waring, 1968; Bloomfield et al., 1974). With BPDE, the isomers that display a more parallel orientation to the base planes, viz., (±)-*syn*- and (−)-*anti*-BPDE, exhibit the largest red-shifts, 10–12 nm, of the long-wavelength absorption relative to free BPDE (Geacintov et al., 1982; Undeman et al., 1983). We have assumed that the shifts can be approximately described by a dispersive interaction mechanism, which gives a sinusoidal dependence on the orientation angle. However, the functional form of the dependence is not found to be very critical, as long as it is monotonic and fulfills the experimental boundary conditions.

Orientational Distribution. For the adducts of all BPDE isomers a significant, qualitatively similar wavelength dependence of LD^r is observed. However, there are quantitative differences regarding both average amplitudes and fine structure. We have concentrated on the spectrum of (+)-*anti*-BPDE bound to poly(dG-dC), since those substances react highly selectively and thus make a suitable model system. Moreover, the low LD^r amplitudes of the other isomers are less informative with regard to orientation. Table II and Figure 4 provide several examples of how the $\langle LD^r \rangle$ value and the $(LD^r_{peak} - LD^r_{trough})$ amplitude rather sensitively depend on the choice of orientational distribution function. The best agreement with experimental LD^r spectra was obtained with the double-Gaussian distribution model, but we shall briefly discuss all four models.

Single Gaussian. This is the expected distribution with a single orientational species and a certain freedom due to Brownian motions. For example, binding of BPDE in the minor groove of unperturbed B-form DNA could be estimated to yield a rather narrow distribution centered roughly around 50° ($\sigma = 10°$). As seen from Figure 4, such a narrow distribution is not compatible with the experimental, large $LD^r_{p/t}$ amplitudes. The best fit with a single Gaussian was obtained with $\alpha_0 = 30°$ ($\sigma = 20°$), but still the agreement with the experimental LD^r spectrum is rather poor, with a too low $\langle LD^r \rangle$.

Two States. Though unphysical, this model demonstrates the effect of two widely separated orientational fractions, giving a more pronounced spectral structure. However, even the best fits were in poor agreement with the observed $LD^r_{p/t}$ and $\langle LD^r \rangle$ values.

Double Gaussian. This may be considered as a hybrid between the two previous models and is a more physical model. The two orientations can be interpreted in terms of two different binding sites or two interchangeable preferred conformations. Of the four simple models applied, this is the only one that can acceptably describe the experimental results. The partition 80%/20% between the two orientation fractions at 20° and 70°, respectively, turned out to be the most successful one from a large number of trials.

Limited Isotropic Domain. This model should correspond to a high angular flexibility, restricted only by steric barriers. It may be considered unphysical in that the mobility is restricted to a plane parallel to the helix axis, but still the model represents a valuable extreme situation and should be essentially correct if the BPDE bond is acting like a hinge. As seen from Figure 4d, however, the simulated spectra are far from agreement with the experimental spectrum.

Before proceeding to a discussion of the results in terms of a structural model of the (+)-*anti*-BPDE–poly(dG-dC) complex, it is appropriate to consider the credibility of the conclusions from the simulations. A possible weakness is our model for the shift of the pyrene chromophore long-wavelength absorption band. A few different monotonic functions, some without physical basis, for the angular dependence of the shift have therefore been tested. However, no great sensitivity to the functional form of the dependence was observed with the present crude distribution models. A basis for the spectral analysis is the assumption of a monotonic shift dependence on the orientation angle, with the boundary states taken from free and "intercalated" BPDE (adducts of predominantly type

I). As there is no experimental evidence for any discrete structures, it seems appropriate to assume that the shift dependence is also continuous. The physical model for the energy dependence on orientation, together with the experimental boundaries for the red-shift, and, finally, the consistency of the simulated results, all support the justification of our model.

Mobility. A number of observations provide evidence that the wide orientational distribution of BPDE is due to mobility of the chromophore long axis relative to that of the DNA helix. First, the absence of any indication of binding heterogeneity (as a function of binding ratio) excludes the possibility of different, covalent binding sites. Second, the fluorescence results prove the existence of different environments for the chromophore, as is also evidenced by the wavelength dependence in LD^r. Furthermore, the observation of excimer fluorescence indicates considerable mobility to allow adjacently bound chromophores to come in close contact with each other. [The excimer formation of BPDE bound to poly(dG-dC) is the subject of a separate study (Eriksson et al., 1988).]

The very low fluorescence polarization anisotropy (FPA) also suggests a rapid mobility of BPDE. Pure pyrene immobilized in a 3-methylpentane glass at 77 K shows a strong positive FPA for the 275-nm (B_b) transition, while there is a certain depolarization in the 300–350-nm (L_a) transition with positive FPA at longer wavelengths and negative FPA at shorter wavelengths (Langkilde et al., 1977). For (+)-*anti*-BPDE bound to DNA, fluorescence lifetime measurements give evidence for at least two different lifetimes [a major fraction at 3.7 ns and a minor one at 45 ns (Undeman et al., 1983)]. The absence of any significant fluorescence polarization anisotropy therefore indicates that depolarization occurs within nanoseconds. This implies a rapid motion of the chromophore relative to the macromolecule [which by itself is expected to have a rotational correlation time of the order of 100 ns or more (Genest et al., 1985)]. A key question is whether this motion occurs within each of the two domains of preferred orientations or if it involves a rapid interchange between them. Although the present data are not sufficient to unambiguously answer this question, the rather narrow orientational distribution within the domain centered at 20° (narrowness evidenced by the high $\langle LD^r \rangle$) makes us strongly favor the latter interpretation. With rapid interchange dynamics it is difficult to believe that the orientation fraction at about 70° is due to true intercalation. No data on residence times in intercalative sites have been reported for covalent DNA adducts; however, with cationic intercalators times of the order of milliseconds have been observed (Wakelin & Waring, 1980).

Conclusions

The results on the structure of the covalent complex between (+)-*anti*-BPDE and poly(dG-dC) presented here may be summarized as follows: (1) *anti*-BPDE considerably impairs the DNA orientation. (2) *anti*-BPDE bound to DNA is characterized by *apparent* angles of ~30° and ~70° relative to the DNA helix for the pyrene z and y axes, respectively. (3) There is a wide orientational distribution of the BPDE z-axis: the results are consistent with a large fraction oriented at approximately 20° relative to the helix axis and a smaller fraction at 70°. (4) The orientational fractions may be interpreted in terms of two interchanging binding conformations.

These observations can now be used to discuss a molecular model for the *anti*-BPDE–DNA adduct. From inspection of molecular models it is seen that binding to the guanine N-2 would preferably lead to accommodation of BPDE in the minor groove of DNA if the B-conformation is retained. However, for steric reasons binding angles smaller than the helical pitch (approximately 50° at a distance of some 7 Å from the helix axis) are then highly unlikely for the pyrene z axis. The observed apparent angle of 30° between the z axis and the helix axis (or the main orientation fraction centered around 20°) is thus in obvious conflict with an unperturbed DNA structure. This conclusion, supported by the observed impaired DNA orientation (due to flexibility or kinks), therefore strongly indicates some kind of local deformation. The small fraction of z axis orientations of (+)-*anti*-BPDE at about 70° may be related to the similar orientation characterizing type I binding [observed with *syn*- and (−)-*anti*-BPDE]. A rapid interchange between the two binding conformations of (+)-*anti*-BPDE, however, makes it unlikely that the orientation fraction at about 70° is due to intercalation.

All evidence indicates the coexistence of (at least) two binding conformations in equilibrium in the (+)-*anti*-BPDE–poly(dG-dC) complex. Also, with the other isomers corresponding conformation equilibria may exist as tentatively indicated by similar dichroism features. In fact, the two conformational states, populated to different extents, may be common to all of the BPDE–DNA complexes. Thus, in the type I binding the 70° conformation should dominate, while the type II binding should be dominated by the conformation at 20°. The latter conformation may be associated with an increased DNA flexibility, explaining why the DNA orientation is seemingly less affected by the (−)-*anti*- and *syn*-BPDE isomers compared to (+)-*anti*-BPDE at the same degree of modification.

Acknowledgments

We thank Prof. Nicholas E. Geacintov for most valuable comments on this work.

Appendix

We shall derive an approximate orientational dependence of the spectral shift caused by dispersive interactions between the BPDE and the DNA chromophores.

Define a Cartesian coordinate system with Z = DNA helix axis and X = dyad axis. If the base planes are assumed to be all in the XY plane, any DNA transition moment vector may be written

$$\mu^i_{DNA} = \mu^i_{DNA}(\cos \phi^i, \sin \phi^i, 0) \quad \text{(A1)}$$

with ϕ^i the angle, in the XY plane, between the transition moment and the X axis. Correspondingly, the transition moment of the pyrene chromophore can be described as

$$\mu_p = \mu_p(\sin \alpha \cos \phi, \sin \alpha \sin \phi, \cos \alpha) \quad \text{(A2)}$$

where α is the angle between μ_p and the DNA helix axis and ϕ is the angle of its projection on the XY plane to the X axis.

We shall assume that the spectral shift, $\Delta\nu$, of the BPDE transition is given by the pairwise dipole–dipole interactions of the nondegenerate transitions of pyrene with the DNA bases (the same interactions as are responsible for dispersive forces)

$$\Delta\nu = \text{const} \times \sum_i V_i \quad \text{(A3)}$$

$$V_i = \mu_p \cdot \mu^i_{DNA}/r_{ip}^3 - 3(\mu_p \cdot \mathbf{r}_{ip})(\mu_{DNA} \cdot \mathbf{r}_{ip})/r_{ip}^5 \quad \text{(A4)}$$

where r_{ip} is the separation vector between the DNA transition moment i and the pyrene transition moment. We may write

$$\mathbf{r}_{ip} = \Delta X \mathbf{e}_X + \Delta Y \mathbf{e}_Y + \Delta Z \mathbf{e}_Z \quad \text{(A5)}$$

with ΔZ the displacement along the helix axis and $\mathbf{e}_Z$ the corresponding unit vector, etc.

Insertion of eq A1, A2, andd A5 into A3 and A4 gives

$$\Delta\nu = \text{const} \times (r^{-3})\mu_p\mu^i_{DNA}\sum_i\{\sin\alpha\cos(\phi^i - \phi) - 3r^{-2}(\Delta X\sin\alpha + \Delta Z\cos\alpha)[\Delta X\cos(\phi^i - \phi) + \Delta Y\sin(\phi^i - \phi)]\} \quad (A6)$$

where r is taken to be an "effective" length of $\mathbf{r}_{ip}$. If we may neglect the second (negative) term in eq A6, which is justified for small off-helix displacements ΔX and ΔY, and assume an effectively homogeneous distribution of DNA transition moments in the XY plane, one obtains simply

$$\Delta\nu = \Delta\nu^\circ \sin\alpha \quad (A7)$$

where the amplitude factor $\Delta\nu^\circ$ will be proportional to the product of the lengths of transition moments of the interacting chromophores and inversely proportional to the cube of the distance of separation. Expressed in wavelength units, by applying the differential relation $d\nu = -cd\lambda/\lambda^2$, one obtains the approximate angular dependence of small red-shifts

$$\Delta\lambda = \Delta\lambda^\circ \sin\alpha \quad (A8)$$

where $\Delta\lambda^\circ$ is the maximum shift (pyrene parallel to bases). In addition to the interaction with the DNA bases, one may also allow for an isotropic "solvent" shift providing

$$\Delta\lambda = \Delta\lambda^{solv} + \Delta\lambda^\circ \sin\alpha \quad (A9)$$

Registry No. (+)-*anti*-BPDE, 63323-31-9; (±)-*anti*-BPDE, 58917-67-2; (±)-*syn*-BPDE, 58917-91-2; (−)-*anti*-BPDE, 63323-30-8; poly(dG-dC), 36786-90-0.

REFERENCES

Alexandrov, K., Rojas, M., Bourgeois, Y., & Chouroulinkov, I. (1983) *Carcinogenesis 4*, 1655–1657.

Birks, J. B. (1980) *Photophysics of Aromatic Molecules*, Wiley, New York.

Bloomfield, V. A., Crothers, D. M., & Tinoco, I., Jr. (1974) *Physical Chemistry of Nucleic Acids*, Harper & Row, New York.

Brookes, P., & Osborne, M. R. (1982) *Carcinogenesis 3*, 1223–1226.

Buening, M. K., Wislocki, P. G., Levin, W., Yagi, H., Thakker, D. R., Akagi, H., Koreeda, M., Jerina, D. M., & Conney, A. H. (1978) *Proc. Natl. Acad. Sci. U.S.A. 75*, 5358–5361.

Cantor, C. R., & Schimmel, P. R. (1980) *Biophysical Chemistry*, Part II, W. H. Freeman, San Francisco.

Chen, F.-M. (1985) *Biochemistry 24*, 6219–6227.

Conney, A. H. (1982) *Cancer Res. 42*, 4875–4917.

Cooper, C. S., Grover, P. L., & Sims, P. (1983) *Prog. Drug Metab. 7*, 295–396.

Davidsson, Å., & Nordén, B. (1976) *Chem. Scr. 9*, 49–53.

Eriksson, M., Jernström, B., Gräslund, A., & Nordén, B. (1986) *J. Chem. Soc., Chem. Commun.*, 1613–1615.

Eriksson, M., Nordén, B., Jernström, B., Gräslund, A., & Lycksell, P.-O. (1988) *J. Chem. Soc., Chem. Commun.* (in press).

Geacintov, N. E., Gagliano, A., Ivanovic, V., & Weinstein, I. B. (1978) *Biochemistry 17*, 5256–5262.

Geacintov, N. E., Gagliano, A. G., Ibanez, V., & Harvey, R. G. (1982) *Carcinogenesis 3*, 247–253.

Geacintov, N. E., Ibanez, V., Gagliano, A. G., Jacobs, S. A., & Harvey, R. G. (1984) *J. Biomol. Struct. Dyn. 1*, 1473–1484.

Gelboin, H. V. (1980) *Physiol. Rev. 60*, 1107–1166.

Genest, D., Mirau, P. A., & Kearns, D. R. (1985) *Nucleic Acids Res. 13*, 2603–2615.

Hogan, M. E., Dattagupta, N., & Whitlock, J. P., Jr. (1981) *J. Biol. Chem. 256*, 4504–4513.

Jeffrey, A. M. (1985) in *Polycyclic Hydrocarbons and Carcinogenesis* (Harvey, R. G., Ed.) pp 187–208, ACS Symposium Series 283, American Chemical Society, Washington, DC.

Jernström, B., Lycksell, P.-O., Gräslund, A., Ehrenberg, A., & Nordén, B. (1983) in *Extrahepatic Drug Metabolism and Chemical Carcinogenesis* (Rydström, J., Montelius, J., & Bengtsson, B., Eds.) pp 469–477, Elsevier, Amsterdam.

Jernström, B., Lycksell, P.-O., Gräslund, A., & Nordén, B. (1984) *Carcinogenesis 5*, 1129–1135.

Koreeda, M., Moore, P. D., Wislocki, P. G., Levin, W., Conney, A. H., Yagi, H., & Jerina, D. M. (1978) *Science (Washington, D.C.) 199*, 778–781.

Langkilde, F. W., Gisin, M., Thulstrup, E. W., & Michl, J. (1983) *J. Phys. Chem. 87*, 2901–2911.

Lycksell, P.-O., Gräslund, A., Ehrenberg, A., Jernström, B., & Nordén, B. (1985) *J. Biol. Chem. 260*, 5857–5859.

MacLeod, M. C., & Zachany, K. (1985) *Chem.-Biol. Interact. 54*, 45–55.

Matsuoka, Y., & Nordén, B. (1982a) *Biopolymers 21*, 2433–2452.

Matsuoka, Y., & Nordén, B. (1982b) *J. Phys. Chem. 86*, 1378–1386.

Meehan, T., & Straub, K. (1979) *Nature (London) 277*, 410–412.

Nakayama, J., Yuspa, S. H., & Poirier, M. C. (1984) *Cancer Res. 44*, 4087–4095.

Nordén, B. (1978) *Appl. Spectrosc. 14*, 157–248.

Nordén, B., & Seth, S. (1979) *Biopolymers 18*, 2323–2339.

Nordén, B., & Seth, S. (1985) *Appl. Spectrosc. 39*, 647–655.

Pelling, J. C., & Slaga, T. J. (1982) *Carcinogenesis 3*, 1135–1141.

Pelling, J. C., Slaga, T. J., & DiGiovanni, J. (1984) *Cancer Res. 44*, 1081–1086.

Pulkrabek, P., Leffler, S., Weinstein, I. B., & Grunberger, D. (1977) *Biochemistry 16*, 3127–3132.

Slaga, T. J., Bracken, W. J., Gleason, G., Levin, W., Yagi, H., Jerina, D. M., & Conney, A. H. (1979) *Cancer Res. 39*, 67–71.

Straub, K. M., Meehan, T., Burlingame, A. L., & Calvin, M. (1977) *Proc. Natl. Acad. Sci. U.S.A. 74*, 5285–5289.

Thulstrup, E. W., Dowing, J. W., & Michl, J. (1977) *Chem. Phys. 23*, 307–319.

Undeman, O., Lycksell, P.-O., Gräslund, A., Astlind, T., Ehrenberg, A., Jernström, B., Tjerneld, F., & Nordén, B. (1983) *Cancer Res. 43*, 1851–1860.

Wada, A., & Kozawa, S. (1964) *J. Polym. Sci. 2*, 853–864.

Wakelin, L. P. G., & Waring, M. J. (1980) *J. Mol. Biol. 144*, 183–214.

Waring, M. J. (1968) *Nature (London) 219*, 1320–1325.

Weinstein, I. B., Jeffrey, A. M., Leffler, S., Pulkrabek, P., Yamasaki, H., & Grunberger, D. (1978) in *Polycyclic Hydrocarbons and Cancer* (Gelboin, H. V., & Ts'o, P. O. P., Eds.) pp 4–36, Academic, New York.